water

MDPI

Article

Rapid Formation and Performance of Aerobic Granular Sludge Driven by a Sodium Alginate Nucleus under Different Organic Loading Rates and C/N Ratios

Chunjuan Gan [1,†], Qiming Cheng [2,†], Renyu Chen [2], Xi Chen [1], Ying Chen [2], Yizhou Wu [1], Cong Li [2], Shanchuan Xu [1] and Yao Chen [2,*]

[1] Municipal Design Research Institute of Chongqing Design Group Co., Ltd., Chongqing 401120, China; jeff-gan@163.com (C.G.); chenxi1@cmrid.com (X.C.); wuyz@cmrid.com (Y.W.); xushanchuan@163.com (S.X.)
[2] School of River and Ocean Engineering, Chongqing Jiaotong University, Chongqing 400074, China; cqming@mails.cqjtu.edu.cn (Q.C.); c18223905496@163.com (R.C.); chenying960114@163.com (Y.C.); CL73@zips.uakron.edu (C.L.)
* Correspondence: chenyao@cqjtu.edu.cn
† These authors contributed equally to this work.

Abstract: The use of aerobic granular sludge (AGS) for wastewater treatment has emerged as a promising biotechnology. A sodium alginate nucleus (SAN) incorporated into the AGS system can enhance aerobic granulation. Two important parameters influencing AGS formation and stability are the organic loading rate (OLR) and C/N ratio. In this study, AGS containing the SAN was cultivated under different OLR and C/N ratios. Through morphological analysis, physicochemical properties, and water quality analysis, the effects of the OLR and C/N ratio on the rapid formation and performance of AGS containing the SAN were investigated. The results showed that the most suitable OLR and C/N ratio in the SAN system were 1.4–2.4 kg/(m^3·d) and 10–15, respectively. A recovery experiment of sodium alginate (SA) showed that the group that formed AGS generally had a higher recovery efficiency compared with the group that did not form granular sludge. This work explored the suitable granulation conditions of AGS containing the SAN, and the results provide a theoretical basis for future practical applications. The recycling of SA as presented in this study may broaden the application prospects of SA.

Keywords: sodium alginate nucleus; aerobic granular sludge; organic loading rate; C/N ratio; formation; performance

Citation: Gan, C.; Cheng, Q.; Chen, R.; Chen, X.; Chen, Y.; Wu, Y.; Li, C.; Xu, S.; Chen, Y. Rapid Formation and Performance of Aerobic Granular Sludge Driven by a Sodium Alginate Nucleus under Different Organic Loading Rates and C/N Ratios. *Water* **2024**, *16*, 1336. https://doi.org/10.3390/w16101336

Academic Editors: Daniela Mesquita and Cristina Quintelas

Received: 9 April 2024
Revised: 3 May 2024
Accepted: 6 May 2024
Published: 8 May 2024

1. Introduction

As one of the most promising biological wastewater treatment technologies, aerobic granular sludge (AGS) has received considerable attention [1–3]. Studies have confirmed that AGS technology exhibits many advantages compared with the conventional activated sludge process, including high settling velocity, high biomass retention, strong microbial structure, simultaneous removal of nitrogen and phosphorus, high tolerance to toxicity, and good ability to handle high organic loading rates (OLRs) [1,2,4]. Consequently, in addition to treating municipal wastewater, AGS has been successful in treating a wide variety of industrial wastewater as well [1,4,5]. However, its widespread application is hampered by several technical bottlenecks, such as a long granulation cycle, complex granulation conditions, and the uncertainty in stable operation and good treatment effects after granulation [1,6]. In addition, the OLR and carbon to nitrogen (C/N) ratio play important roles in the formation and stability of aerobic granules during the granulation process [6,7]. Therefore, it is imperative to explore a cultivation method that can quickly form AGS and maintain its stable structure and performance, with the overarching goal of broadening the application of AGS.

Sodium alginate (SA), a naturally occurring polyanionic polysaccharide derived from marine brown algae, is composed of a sequence of 1–4 glycosidic linkages connecting blocks of α-L-guluronic acid (G) and β-D-mannuronic acid (M) monomers [8]. Because of its biocompatibility, SA promotes biological adhesion and can be converted into a stable gel state with strong adhesive properties towards microbes [9–11]. This suggests its potential use as a nucleation site for sludge formation and microbial attachment to facilitate the development of granular sludge structures [12]. In our previous study [13], the rapid formation of AGS was realized through the preparation of a sodium alginate nucleus (SAN), which resulted in the formed AGS having good sedimentation performance and pollutant removal ability. However, that study mainly focused on the feasibility and mechanism of a SAN to cultivate AGS, ignoring the influence of operational parameters on the formation and performance of AGS, which is the focus of this study. It should be noted that AGS formation, characteristics, and stability are affected by the OLR. Moy et al. suggested that AGS was irregularly shaped and had folds, depressions, and crevices at a high OLR of 9 kg COD/(m^3·d) [14]. Similarly, Corsino et al. found that at a high OLR of 7–15 kg COD/(m^3·d), the formed AGS was characterized by filamentous structures and a black-colored core [15]. However, low or fluctuating OLRs can cause filamentous bacteria to proliferate within granules, leading to loose and porous granular structures [6]. It has been reported that filamentous bacteria proliferate when the OLR is too low, resulting in loose, porous structures and ultimately deteriorating the stability of the AGS structure [14,16]. Meanwhile, given the lack of nutrients, the biological activity in the reactor is low, and thus, sewage treatment efficiency cannot be guaranteed. However, although AGS is formed at a high OLR, it easily loses its stability under high OLRs [3,6,17,18]. This may be attributed to the fact that a high OLR accelerates the metabolism and excessive secretion of extracellular polymers (EPS), which changes the ratio of protein (PN) to polysaccharides (PSs) in the extracellular polymers [1,17]. Overall, the above studies have demonstrated that the OLR is one of the most important parameters affecting AGS.

One of the main challenges for AGS application is that its long-term stability is affected by several factors, such as C/N. Zhang et al. found that large granules, with a size of 650 μm and compact structure (integrity coefficient < 0.1), had a lower C/N influent compared with disintegrated granules with a high influent C/N [19]. Studies have also suggested that by reducing C/N, it would be possible to enrich nitrifying bacteria and increase their tolerance to high ammonia levels [20,21]. However, when operating for a long period of time, extremely low C/N wastewater would cause the granular structure to collapse [6,22]. Despite the fact that a high or low C/N is unfavorable for AGS formation, low-C/N wastewater (less than 1) with high ammonia nitrogen levels can still be treated with matured AGS that maintains good structural stability and denitrification ability despite high concentrations of ammonia nitrogen [23]. Because of its unique layering structure, AGS can easily undergo simultaneous nitrification and denitrification inside granular sludge under high levels of dissolved oxygen (DO), thereby effectively reducing the demand for carbon sources [6]. Notably, this feature of AGS gives it broad application prospects in the treatment of sewage with a low C/N ratio [24–26]. Therefore, we hypothesize that two operational parameters (the OLR and C/N) can further affect the rapid formation and performance of AGS driven by the SAN.

In the present study, different OLRs and C/N ratios were designed, and then their effect on the rapid formation of AGS in a SAN system was explored. Based on the previous study [13], the optimal dosage of the SAN was put in a sequencing batch reactor (SBR), followed by monitoring the properties and performance of AGS, including the granular morphological structure, EPS content, and water quality. To better realize practical applications, the recovery efficiency of sodium alginate (SA) was also analyzed. It is expected that our findings will provide a theoretical basis for future practical applications of the SAN.

2. Materials and Methods

2.1. Preparation of the Sodium Alginate Nucleus (SAN)

The SAN was prepared by cross-linking a $CaCl_2$ solution (20 g/L) and SA (20 g/L, chemically pure, Xilong Scientific, Shantou, China). A magnetic agitator (78-1, Dingxinyi Instrument, Shenzhen, China) was used to complete the cross-linking reaction (see the previous study [13] for details). A SAN with a certain mechanical strength and a spherical shape was prepared through the hydraulic shear force generated by the liquid-swirling flow. The prepared SAN was soaked in pure water for 12 h, dried at 40 °C for 18 h, and then weighed.

2.2. Batch Experiment

This study used nine groups of identical SBRs (5 × 75 cm) with a 1 L working volume (Figure 1). The reactors were operated with a cycle of 24 h, including a feeding phase (5 min), aeration phase (23 h), settling phase (5 min), discharge phase (5 min), and an idle phase (45 min). The temperature of the reactors was controlled at around 25 °C, and peristaltic pumps (DIPump 550, Kamoer Fluid Tech, Shanghai, China) were used to discharge effluent from the 500 mL scale line of the reactor with a volumetric exchange ratio of 50%. During the aeration phase, an airflow rate of 1.5 cm/s was set to provide the DO and hydraulic shear force through the aeration device located at the bottom of the reactor. Flocculent sludge with poor settling performance was removed during the setting phase. In addition, the dosage of the SAN was controlled at 0.06 g/L, as reported previously [13].

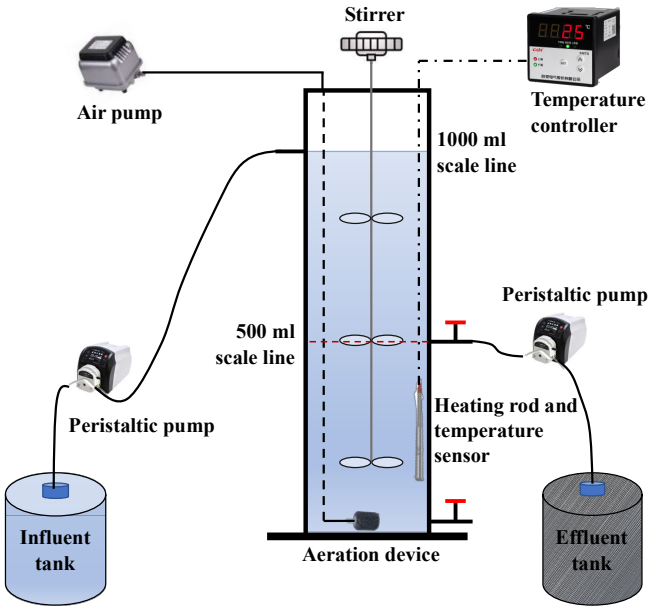

Figure 1. Schematic diagram and operation cycle of the SBR.

A two-phase experiment was conducted in this study. In phase 1 (P1), synthetic piggery flushing wastewater with different OLR values (0.8–1.0 kg/(m^3·d), 1.4–1.6 kg/(m^3·d), 2.2–2.4 kg/(m^3·d), 2.8–3.0 kg/(m^3·d), and 5.5–6.0 kg/(m^3·d)) was added into the five groups of reactors (labeled P1-R1, P1-R2, P1-R3, P1-R4, and P1-R5). In phase 2 (P2), four groups of reactors (P2-R1, P2-R2, P2-R3, and P2-R4) with different C/N ratios were designed. The C/N ratios were 10 ± 1, 15 ± 2, 25 ± 2, and 30 ± 3, respectively. The P1 experiment and the P2 experiment were performed in triplicates for replication purposes.

2.3. Seed Sludge and Wastewater Characteristics

Inoculated sludge was sourced from the Wanzhou Wastewater Treatment Plant in Chongqing, China. Dark brown in color, the seed sludge was loose and flocculent. The sludge volume index (SVI_{30}), the concentration of mixed liquor suspended solids (MLSSs), and the

specific oxygen uptake rate (SOUR) were 160 mL/g, 1 g/L, and 13.61 mg O_2/(g MLVSS·h), respectively. The PN and PS content were 8.064 mg/g MLSS and 4.410 mg/g MLSS, respectively.

The synthetic piggery flushing wastewater was prepared before each experiment. The detailed composition is shown in Table 1 according to some typical flushing wastewater collected from breading pig farms [27–29]. Anhydrous sodium bicarbonate was also used as a buffer, adjusted to a pH of 7–7.5. The buffer was used to ensure higher biological activity and increase the operational stability of the AGS [15]. Ammonium chloride was used as the main nitrogen source, whereas monopotassium phosphate was applied as the only phosphorus source. It was previously reported that calcium chloride (Ca^{2+}) and magnesium sulfate (Mg^{2+}) can promote AGS formation and structural stability by bridging and neutralizing negative charges to reduce electrostatic repulsion [30]. Therefore, 111 mg/L $CaCl_2$ and 260 mg/L $MgSO_4$ were added to the synthetic wastewater. The concentration of chemical oxygen demand (COD) with glucose, yeast, and anhydrous sodium bicarbonate as the carbon source in P1 and P2 was 900–6000 and 1250 mg/L, respectively. In addition, the concentration of NH_4^+-N was 70 and 44–110 mg/L and total nitrogen (TN) was 80 and 50–130 mg/L in P1 and P2, respectively. However, total phosphorus (TP) was 11 mg/L in P1 and P2.

Table 1. The synthetic piggery flushing wastewater.

Ingredients	Concentration (mg/L)	
	P1	P2
$C_6H_{12}O_6$	600–4800	1000
NH_4Cl	250	154–385
KH_2PO_4	50	50
$NaHCO_3$	750	450–1150
$CaCl_2$	111	111
$MgSO_4$	260	260
EDTA	21	21
Yeast	100	100
$ZnSO_4 \cdot 7H_2O$	0.12	0.12
H_3BO_3	0.11	0.11
$CuSO_4 \cdot 5H_2O$	0.05	0.05
$MnCl_2 \cdot 4H_2O$	0.12	0.12
$CoCl_2$	0.17	0.17
$H_8MoN_2O_4$	0.1	0.1
$FeSO_4 \cdot 7H_2O$	0.16	0.16

2.4. Analysis Methods

COD, NH_4^+-N, TN, TP, SVI_{30}, MLSSs, and mixed liquid volatile suspended solids (MLVSSs) were measured according to standard methods [31]. The settling velocity of AGS was measured according to the static sedimentation method. Briefly, the selected sludge was allowed to settle in a measuring cylinder labeled as the distance marker. The settling distance of the AGS interface after *t* min was monitored. Sludge particles were randomly collected and washed three times, and the particle size distribution (PSD) of AGS was determined using ImageJ (Version 1.50b) software. A mature AGS was randomly selected from each reactor for pretreatment and then placed under a scanning electron microscope (SEM, Zeiss Sigma 300, Carl Zeiss AG, Oberkochen, Germany) for microscopic examination.

The DO concentration was measured using a DO meter (HACH HQ30d, Hach Company, Loveland, CO, USA). Next, the DO time was plotted to obtain the OUR (mg O_2/h) based on the slope. SOUR (mg O_2/(g MLSS·h) or mg O_2/(g MLVSS·h) was calculated as in Equation (1).

$$\text{SOUR} = \frac{\text{OUR}}{\text{MLSS}} \text{ or SOUR} = \frac{\text{OUR}}{\text{MLVSS}} \quad (1)$$

where SOUR represents the specific oxygen uptake rate, mg O_2/(g MLSS·h) or mg O_2/(g MLVSS·h); OUR represents the oxygen uptake rate, mg O_2/(L·h); MLSS represents the

concentration of the mixed liquor suspended solids, g/L; and MLVSS represents the concentration of the mixed liquid volatile suspended solids, g/L.

The EPS was extracted using the modified centrifugation method for subsequent characterization. The PN content in the extracted EPS was determined using the Coomassie brilliant blue staining method, and PS was measured using the anthrone–sulfuric acid method. The PN and PS contents were then measured using a UV spectrophotometer (HACH DR6000, Hach Company, Loveland, CO, USA) at 595 nm and 575 nm, respectively. The details of EPS extraction and analysis were presented in a previous study [13].

3. Results and Discussion

3.1. The Effect of Different OLRs on AGS

3.1.1. Morphological Changes in AGS under Different OLRs

On the seventh day of granulation, AGS was observed in some groups but exhibited different morphologies in the different OLR systems. In the P1-R1 group, AGS dominated in the reactor without flocculent sludge, and the sludge particles had clear edges, uniform particle size, and dense surfaces. The granulation was the best among the five groups. In the P1-R2 group, most were granular sludge, with a small amount of flocculent sludge. The group had a good granulation effect. The results indicated that activated sludge can be granulated rapidly in a short time (7 days) with a lower OLR (<1.6 kg/(m^3·d)). The proportions of granular sludge and flocculent sludge in the P1-R3 group were about half each, and the granulation decreased with an increase in the OLR. Granular sludge accounted for a relatively small amount (lower than 20%) in the P1-R4 and P1-R5 groups. However, there was granular sludge with clear edges and large particle size in the P1-R5 group, which could have resulted from the sludge that had accumulated on the inner wall of the reactor, and not the AGS with SA as the nucleus. In addition, the effluent of the reactor was turbid. The results indicated that a high OLR was not suitable for the rapid formation of granular sludge, which may be attributed to the fact that microorganisms produced a large number of organic acids under high organic loading, thereby promoting the reproduction of filamentous bacteria [32]. Consequently, excessive filamentous bacteria had difficulty adhering to the surface of the SAN [13]. Moreover, some filamentous bacteria grew from the inside of AGS, thereby destroying the sphere structure and stability of the AGS, and ultimately causing the disintegration of the AGS [6,33]. Notably, our results were consistent with previous studies. For example, one study found that once AGS grew larger, it became unstable because of filamentous microbial growth [18]. In addition, Chen et al. revealed that when filamentous bacteria predominated in granules, excessive filaments disrupted the structural integrity [34], leading to granule fragmentation.

Because of the low granulation of sludge (granulation rate < 20%) in the P1-R4 and P1-R5 groups, the micromorphology of the AGS focused on the other three groups. Figure 2 shows the SEM results of the AGS in the P1-R1, P1-R2, and P1-R3 groups. The results showed that the inside of the granules had rich biological species with different morphological features, including rod-shaped, spherical, and filamentous morphologies. The P1-R1 group, with the lowest OLR, was dominated by rod-shaped and spherical bacteria, without free filamentous bacteria (Figure 2a), and the surface of the AGS was dense and full. This may be attributed to the presence of cocci and bacilli cells, which compacted the granular surface [13,33]. Free filamentous cells occurred on the surface and inside of the AGS in P1-R2 (Figure 2b), with the proportion of bacilli and filamentous cells each accounting for about 50%. The density of the AGS cultured in this group was lower than that in the P1-R1 group, the cell structure was relatively loose, and part of the structure was connected by the bridging and netting of filamentous bacteria. This result was consistent with previous studies, which indicated that bacteria with filamentous structures can serve as skeletons for free cells by bridging and trapping them [13,35]. In addition, bivalent metal ions (Ca^{2+} and Mg^{2+}) can be combined with EPS secreted by microbes to form EPS–Ca^{2+}(Mg^{2+})–EPS bridge structures, allowing for the interconnection of microbial cells with inorganic substances [13]. There were a lot of cavities in the AGS in P1-R3 (Figure 2c). Both the looseness degree

of particles and the proportion of filamentous bacteria further increased, and this might be an advantage to mass-transfer metabolites, nutrients, and oxygen within large-sized granules [36]. With an increase in the OLR, the proportion of filamentous bacteria in AGS increased, whereas the sludge particles tended to loosen. Based on the analysis of the SEM results, a low OLR was more conducive to the rapid formation of AGS with a compact structure. In contrast, the excessive growth of filamentous cells resulted in the continuous breakage of granules, finally causing the failure of granulation under a high OLR (above 2.8 kg/(m^3·d)).

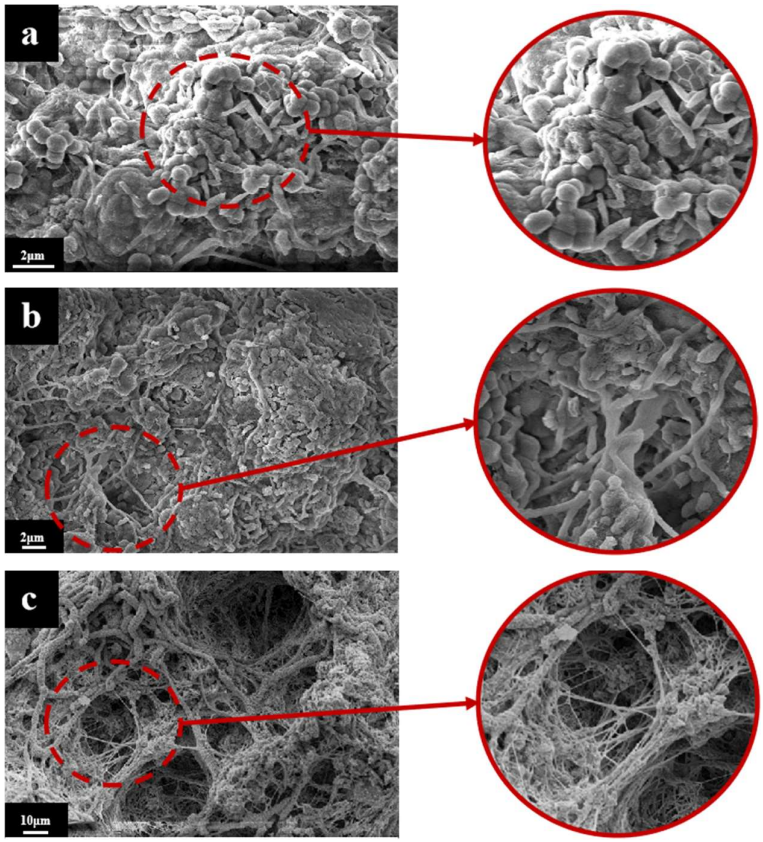

Figure 2. SEM images of the internal structure of granules in (**a**) P1-R1, (**b**) P1-R2, and (**c**) P1-R3 during the stabilization phase under varying OLRs.

3.1.2. Physicochemical Properties of AGS under Different OLRs

Based on Figure 3a, it was evident that the MLSS concentration in the P1 system showed an overall upward trend with the increase in the OLR, which may be ascribed to the sufficient carbon source. It is well known that biological activity and reproductive rate are positively correlated with nutrients. Figure 3b shows that the settling velocity of sludge particles in each system gradually decreased with the increase in the OLR, which was opposite to the MLSS concentration. This may be attributed to the intensified friction between the particles with the increased MLSS concentration [37]. Although the settling velocity was obviously negatively correlated with the OLR and the sludge concentration, especially in the P1-R1, P1-R2, and P1-R3 groups, they still maintained excellent sedimentation performance. Notably, the settling velocity could reach 45 m/h, 35 m/h, and 30 m/h, respectively. In addition, the fast-settling bacteria stayed in the reactor, whereas the poorly settling flocs were washed out, thereby enhancing granulation [6,38]. Therefore, the granulation effect in the P1-R1, P1-R2, and P1-R3 groups was better. In summary, it was evident that mature AGS could be quickly cultivated under a lower OLR (0.8–2.4 (kg/m^3·d)) with the addition of a SAN, and the AGS had better sedimentation performance and complete structure. On the other hand, an excessively high OLR (≥5.5 kg/(m^3·d)) would cause

excessive growth of microorganisms, especially filamentous bacteria that are not conducive to sludge aggregation and AGS cultivation.

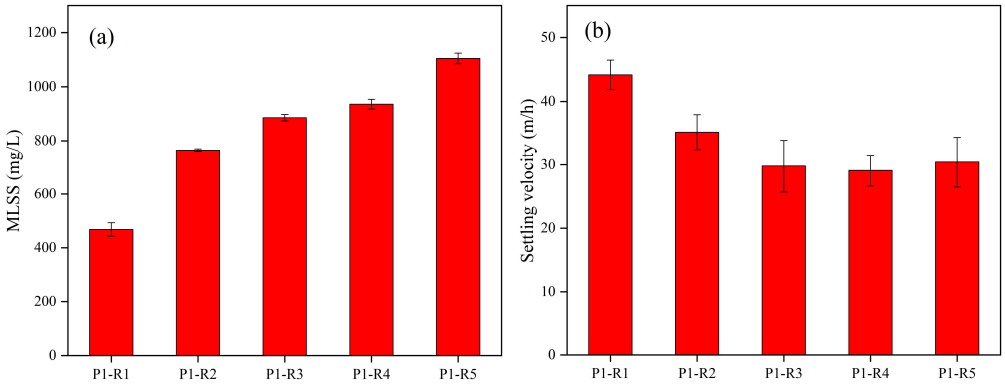

Figure 3. (**a**) MLSS concentration and (**b**) settling velocity of sludge in the P1-R1, P1-R2, P1-R3, P1-R4, and P1-R5 groups under varying OLRs.

When the OLR increased from 0.8 to 2.4 kg/(m^3·d), there was an increase in the proportion of large granules and their average particle size (Figure 4). The results showed that the average particle size of the P1-R1 group was about 1.2 mm, the particle size of the P1-R2 group was concentrated around 1.6 mm, and the average particle size in the P1-R3 group rose to about 2.3 mm. Combining the AGS formation results, it was found that the higher the OLR, the larger the granules formed, and thus, it was not beneficial to granulation. This may be due to the growth of the anaerobic core inside the granules. Previous studies have demonstrated that there was a maximum depth of 500 µm to which DO could penetrate [39,40]. Moreover, the granular strength and cohesion between cells decreased with the appearance of anaerobic cores [18], which could result in the disintegration of granules. This study found that granule particle sizes gradually increased with an increasing OLR, resulting in large granules becoming unstable, and AGS stability was adversely affected, which was consistent with previous studies [13,32,41].

The EPS of the sludge was measured in the P1-R1, P1-R2, and P1-R3 groups on the fifth day (granulation period), tenth day (mature period), and fifteenth day (aging period), and the obtained results are shown in Figure 5. The EPS content of each group showed a rising trend between the 5th day and the 10th day, and then it exhibited a decreasing trend in the following period. As a result of the microorganisms secreting EPS during the granulation process, AGS formation was promoted [42–44]. However, after the mature period, AGS secreted less EPS. This may be due to the limitation of sludge discharge and the proliferation of microorganisms, which caused the DO concentration to decrease and resulted in an insufficient carbon source. The former led to a reduction in microbial activity and EPS secretion, whereas the latter led to the consumption of EPS as energy supply by microorganisms, which also caused a decrease in the EPS content.

During each period, the EPS content showed an upward trend with the increase in the OLR. In addition, it was found that the effect of the OLR on the PS content was more significant than that on the PN content. With an increase in the OLR, the PS content, which has a large number of hydrophilic groups [43,45], increased significantly, whereas the PN content, which is mainly hydrophobic amino acids [43,45], was less affected. Therefore, PN/PS showed a downward trend as the OLR increased and the hydrophilicity of the sludge increased. This result was consistent with the shape characteristics of granular sludge with a larger particle size and a looser surface. Collectively, the results demonstrated that a high OLR promoted the secretion of PS and the PN/PS in AGS showed a downward trend and destroyed the hydrophobicity and surface electronegativity, which was consistent with the findings of a previous study [17]. Therefore, it was more difficult to gather and adsorb on the SAN, which caused the bacterial micelles to disintegrate and degenerate into loose sludge. In summary, in the granulation range, a lower OLR (0.8–2.4 kg/(m^3·d))

was more conducive to the rapid formation of stable AGS with uniform particle size and compact structure.

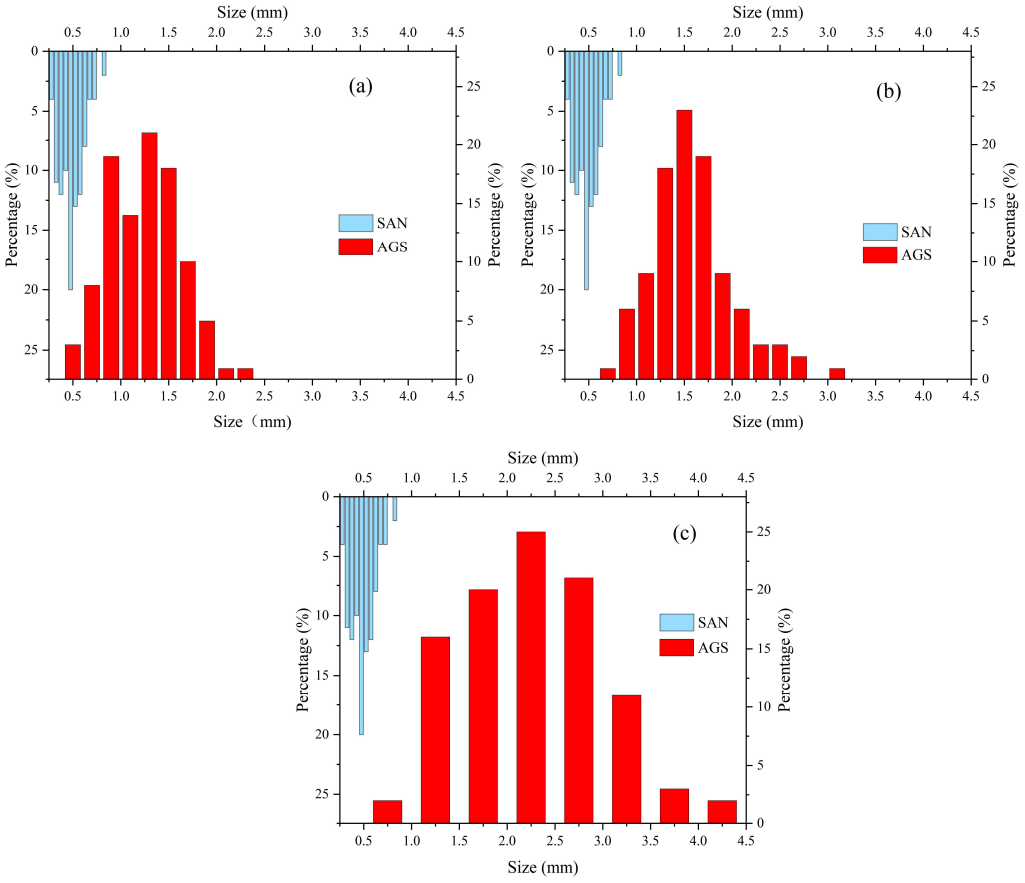

Figure 4. Particle size distribution of mature AGS in (**a**) P1-R1, (**b**) P1-R2, and (**c**) P1-R3 under varying OLRs.

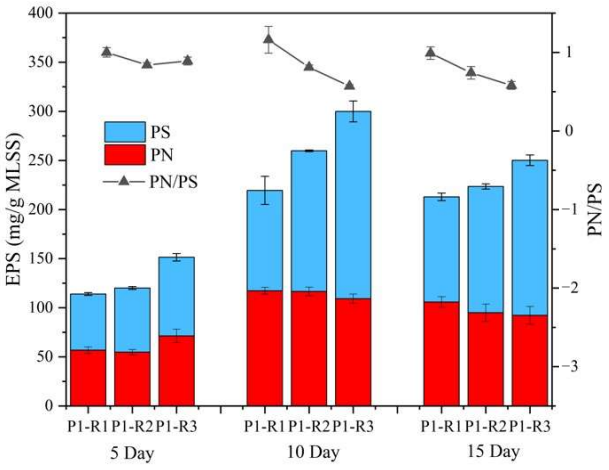

Figure 5. Variation in the PN and PS contents in P1-R1, P1-R2, and P1-R3 during granulation with varying OLRs.

3.1.3. Overall Performances during the Granulation Period under Different OLRs

Figure 6a shows the COD removal efficiency of different OLRs. The COD removal efficiency in the P1-R5 group was the worst, at only about 60%. When the OLR was below 3.0 kg/(m^3·d), the COD removal efficiency improved significantly, where the average removal efficiency rose by 30%. However, when the OLR was as low as 0.8 kg/(m^3·d)

(P1-R1), the COD removal efficiency decreased. These results suggested that a too low or a too high OLR would have an adverse effect on COD removal efficiency. Iorhemen and Liu reported that high organic carbon sources inhibited the substrate utilization of microorganisms, and too low OLRs also inhibited the activity of microorganisms [3]. In addition, results showed that the COD removal efficiency was relatively stable and reached its best when the OLR was in the range of 1.4–2.4 kg/(m^3·d).

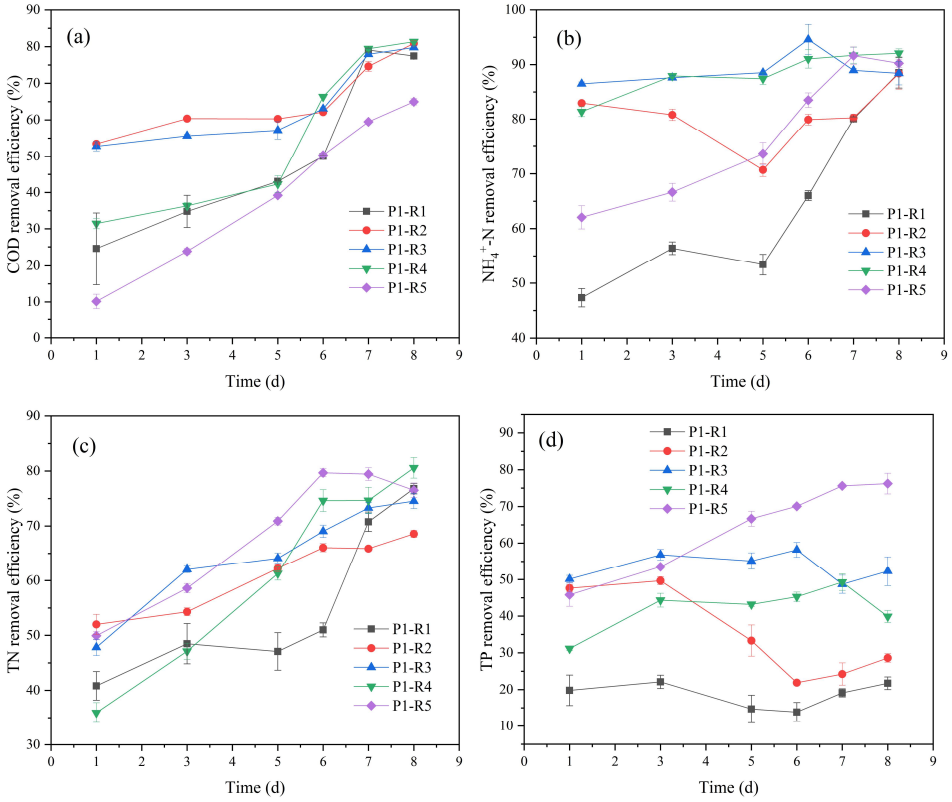

Figure 6. (**a**) Variations in COD removal efficiency, (**b**) NH_4^+-N removal efficiency, (**c**) TN removal efficiency, and (**d**) TP removal efficiency under varying OLRs.

Figure 6b shows the NH_4^+-N removal efficiency of different OLRs. The OLR had an impact on the NH_4^+-N removal efficiency during the adaptation period. The results revealed that the overall NH_4^+-N removal efficiencies in the P1-R3 and P1-R4 groups were stable at 85–95%, whereas the NH_4^+-N removal efficiencies in the P1-R1, P1-R2, and P1-R5 groups were low (50–70%), which may be because the OLR was too low. Although AGS was formed, the nutrient substrate was insufficient, which lowered the microbial activity. Moreover, considering that nitrifying bacteria are chemoautotrophic microorganisms, excessively high OLR conditions enhance the growth and reproduction of heterotrophic bacteria in large numbers because they are able to compete with nitrifying bacteria for nutrients [46]. Consequently, nitrifying bacteria cannot become the dominant species, and thus, the nitrification is limited, thereby resulting in a poor NH_4^+-N removal efficiency. In addition, given that the OLR had almost no effect on the NH_4^+-N removal efficiency during the mature period, the five groups could reach about 90% efficiency. The reason may be that the nitrifying bacteria accumulated sufficiently, and the substrate was no longer the main factor limiting the nitrification.

Figure 6c shows the TN removal efficiency of different OLRs. During the adaptation period, the TN removal efficiencies in the P1-R2 and P1-R3 groups were stable and great. This may be ascribed to the anoxic/anaerobic zones inside the AGS [47,48], which resulted in excellent denitrification performance [49]. It is worth noting that the TN removal efficiency in P1-R5 was the best, which may be due to the fact that a high OLR was beneficial to the denitrifying bacteria [50]. In the high OLR system, the sludge particles

shed from the inner wall of the reactor, thereby resulting in a micro-local DO gradient, which improved the efficiency of the denitrification process. In addition, during the mature period, the TN removal efficiency in the P1-R5 group decreased, whereas the other groups exhibited an upward trend. This may be attributed to the slower but more stable AGS granulation and maturation. Simultaneously, the aging and disintegration were slower, which was conducive to longer-term and stable water treatment. Overall, these results suggest that the OLR in the range of 2.2–2.4 kg/(m^3·d) was more conducive to sludge granulation and denitrification performance.

Figure 6d shows the TP removal efficiency of different OLRs. TP removal efficiency was significantly affected by the OLR, showing a rising trend with an increase in the OLR. In the P1-R1 group, the TP removal efficiency was only 25%, whereas in the P1-R5 group, the TP removal efficiency rose to 80%. This may be attributed to the high biological activity provided by sufficient carbon sources; thus, the full reaction took place and achieved high-efficiency TP removal. It is worth mentioning that the TP removal efficiency decreased in the later stage. The reasons were as follows: (1) during the experiment, there was almost no sludge discharge from the reactors; therefore, TP adsorbed on the sludge was not removed in time, thereby resulting in poor TP removal efficiency; (2) in the later stage, the DO was insufficient, part of the sludge was disintegrated, and phosphorus was released; thus, the TP removal efficiency was reduced. Although phosphorus can be removed via precipitation with Ca^{2+} and Mg^{2+}, the pH values of all reactors were controlled at 7.0–7.5, resulting in the ignorance of chemical phosphorus removal.

3.2. The Effect of Different C/N Ratios on AGS

3.2.1. Morphological Changes in AGS under Different C/N Ratios

Figure 7 shows the AGS formation in the four groups of different C/N systems by the seventh day. In the P2-R1 and P2-R2 groups, almost all were yellow AGS, with no flocculent sludge, and the sludge particles had clear edges, uniform particle size, and dense surfaces. In addition, the effluent was clear. In the P2-R3 group, the proportions of light yellow AGS and flocculent sludge were about half each, and the sludge particle size was uneven. In the P2-R4 group, the system was dominated by flocculent sludge, and the effluent was turbid. These results indicated that a high C/N ratio was not suitable for the formation of granular sludge. Notably, the reason is the same as that described in the previous section, where high C/N promoted the reproduction of filamentous bacteria [32], which destroyed the sphere structure and stability of the AGS and caused the disintegration of the AGS [33].

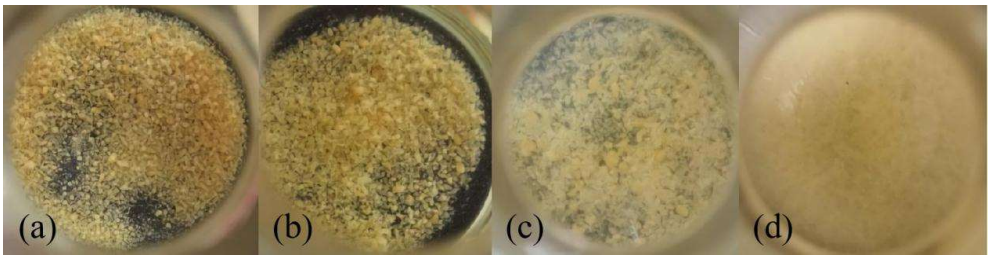

Figure 7. Morphology observations of sludge in (**a**) P2-R1, (**b**) P2-R2, (**c**) P2-R3, and (**d**) P2-R4 under varying C/N ratios.

According to the granular rate of each group, the micromorphology of AGS was only studied in the two groups with C/N ratios of 10 ± 1 and 15 ± 2. Figure 8 shows the SEM results of the AGS in the P2-R1 and P2-R2 groups. The granules also had various microbes inside, including rod-shaped, spherical, and filamentous morphologies. The difference in the sludge extracted in the two systems was small. The content and distribution of filamentous cells were less affected by C/N: when C/N was controlled by the NH_4^+-N concentration, and the organic matter content remained unchanged. Based on the results, it was evident that the suitable C/N ratio for rapid granulation was within the range of 10–15.

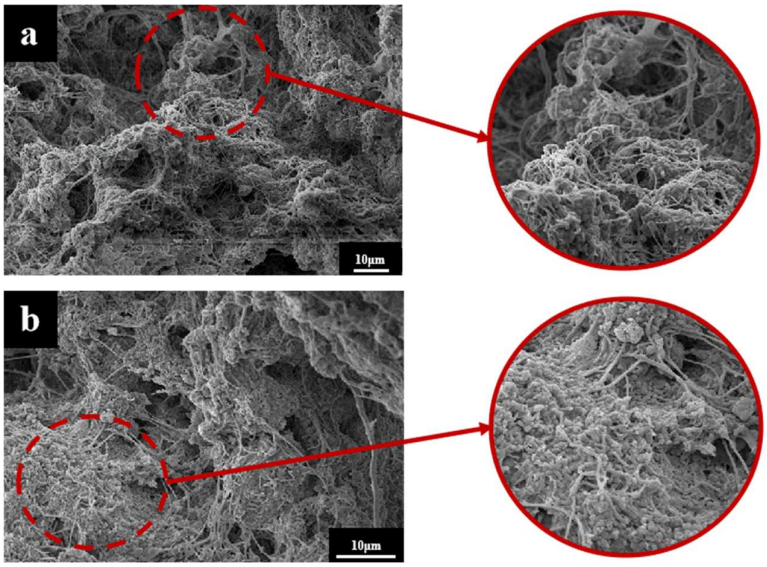

Figure 8. SEM images of the internal structure of granules in (**a**) P2-R1 and (**b**) P2-R2 at the stabilization phase under varying C/N ratios.

3.2.2. Physicochemical Properties of AGS under Different C/N Ratios

Figure 9 shows that the MLSS concentration and settling velocity in the P2-R2 group were the highest in each group, indicating that the microbial activity and the ability to form AGS in P2-R2 were better than in the other groups. When C/N decreased, excessively high free ammonia concentration would inhibit microbial activity [51], thereby causing a drop in the MLSS concentration. Using a higher C/N, the activity and reproduction of microorganisms were significantly reduced because of the insufficient nitrogen source for the synthesis of cell proteins, thereby resulting in the obstruction of sludge accumulation. Figure 9b shows that the settling velocity of sludge particles in the P2-R1 group was about 35 m/h compared with 40 m/h in the P2-R2 group. Although there was a certain drop, it was still far better than traditional flocculent-activated sludge, which indicated the superiority of granular sludge in terms of sedimentation performance. Altogether, these results suggested that mature AGS could be quickly cultivated under lower C/N (C/N = 10–15) with the addition of the SAN, and the AGS had better sedimentation performance and complete structure.

Figure 10 shows the particle size of AGS with a high granular rate and the initial SAN size. The average particle size of the P2-R1 group was about 1.9 mm, whereas the particle size of the P2-R2 group was concentrated around 1.3 mm. The results indicated that a C/N in the range of granulation (10–15) had little effect on the granulation. Therefore, both systems realized the efficient formation of AGS and maintained the stability of the AGS structure during operation. According to Zhou et al., AGS stability was adversely affected by the large size of granules [52], which explained the uniformity in the particle size and the excellent sedimentation performance in the P1-R2 group.

The EPS of the sludge was measured in the P2-R1 and P2-R2 groups on the fifth day (granulation period), tenth day (mature period), and fifteenth day (aging period), and the obtained results are shown in Figure 11. The EPS content of each group showed a rising trend between the 5th day and the 10th day, and then it exhibited a decreasing trend in the following period, which was similar to the OLR result. In addition, during each period, C/N in the range of granulation had no significant effect on the EPS content and PN/PS. The EPS content and PN/PS in the P2-R2 group were slightly higher, which was consistent with the granulation and particle size results. It is worth noting that as C/N increased, PN, which is mainly hydrophobic amino acids, increased, whereas PS (with a large number of hydrophilic groups) was almost unaffected. Notably, this result was opposite to that of the OLR, which may be explained by the fact that C/N was only adjusted according to the nitrogen source without changing the carbon source. It was found that excessive free

ammonia limited the aggregation of functional microbes and could reduce the secretion of PN, which was consistent with previous studies [53]. Taken together, these results suggest that, in the granulation range (C/N = 10–15), a higher C/N was more conducive to the formation of stable AGS.

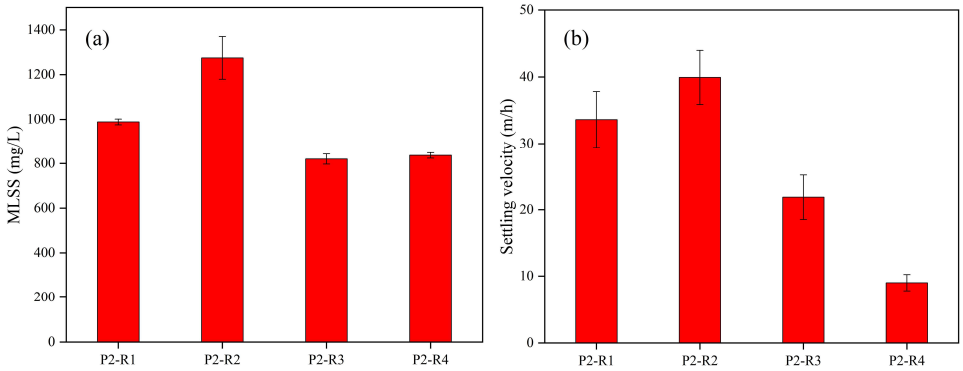

Figure 9. (**a**) MLSS concentration and (**b**) settling velocity of sludge in P2-R1, P2-R2, P2-R3, and P2-R4 groups under varying C/N ratios.

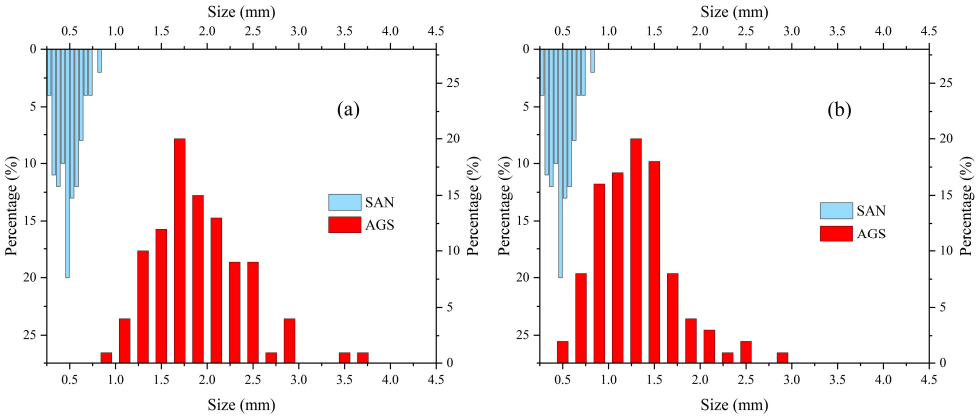

Figure 10. Particle size distribution of mature AGS in (**a**) P2-R1 and (**b**) P2-R2 under varying C/N ratios.

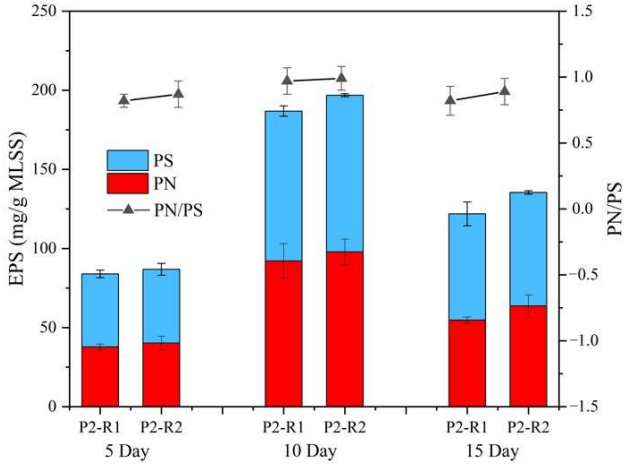

Figure 11. Variation in PN and PS contents in P2-R1 and P2-R2 groups during granulation with varying C/N ratios.

3.2.3. Overall Performances during the Granulation Period under Different C/N Ratios

The COD removal efficiency of different C/N ratios is shown in Figure 12a. During the granulation period, the COD removal efficiency in the P2-R1 and P2-R2 groups was

about 60–65%, and the efficiency rose to about 80% during the mature period, which was higher than the P2-R3 and P2-R4 groups. The results indicated that a too high C/N ratio would have an adverse effect on COD removal efficiency. High organic carbon sources hindered AGS granulation and inhibited substrate utilization by microorganisms [3]. Based on the results, the COD removal efficiency was the best when C/N was in the range of 10–15.

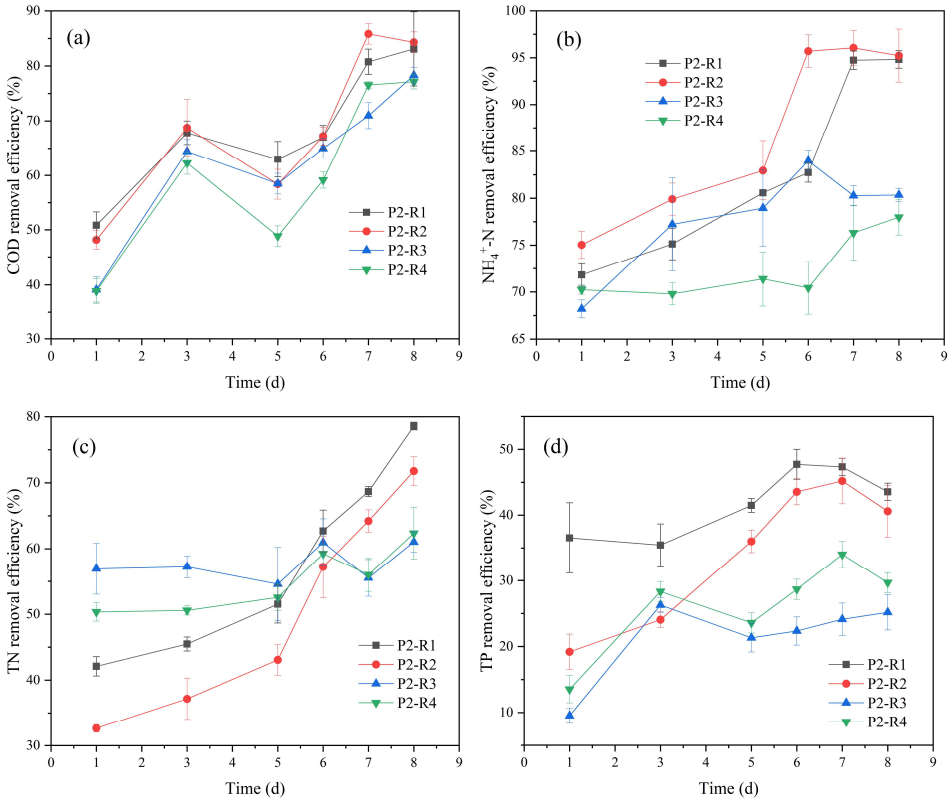

Figure 12. (**a**) Variations in COD removal efficiency, (**b**) NH_4^+-N removal efficiency, (**c**) TN removal efficiency, and (**d**) TP removal efficiency under varying C/N ratios.

Figure 12b shows the NH_4^+-N removal efficiency of different C/N ratios. It was evident that the removal efficiency of the lower C/N group (P2-R1 and P2-R2) was significantly better than that of the higher C/N group (P2-R3 and P2-R4). Moreover, NH_4^+-N removal efficiency was best when C/N was about 15, which could reach more than 95%. This may be attributed to the fact that excessively high free ammonia concentration inhibited the activity of nitrifying bacteria [54], thereby resulting in a decrease in NH_4^+-N removal efficiency, which was consistent with a previous study [55]. In addition, Liu et al. revealed that nitrifying bacteria cannot become the dominant species under a too high C/N ratio [46]. Therefore, nitrification was limited, ultimately resulting in poor NH_4^+-N removal efficiency.

The TN removal efficiency of different C/N ratios is shown in Figure 12c. Given the insufficient nitrogen source during the adaptation period, the development of AGS was lagging, and the TN removal efficiency was low in the P2-R1 and P2-R2 groups. However, as the granulation and particle size increased during the mature period, the anoxic/anaerobic zone inside the AGS increased [47,48], which enhanced the denitrification, and, eventually, the TN removal efficiency increased to 70–80%. In addition, the higher C/N group (P2-R3 and P2-R4) provided a sufficient carbon source for denitrification [50], and thus, the TN removal efficiency was better than in the lower C/N group (P2-R1 and P2-R2) in the adaptation period. However, from the mature period, it remained stable, with a difference

of less than 10%. In conclusion, these results indicated that C/N in the range of 10–15 was more conducive to sludge granulation and denitrification performance.

Figure 12d shows the TP removal efficiency of different C/N ratios. The results indicated that the overall TP removal efficiency was poor during the experiment, and the TP removal efficiency was higher in the P2-R1 and P2-R2 groups compared with the P2-R3 and P2-R4 groups. The insufficiency of DO and the inability to discharge sludge were the main reasons [56]. Furthermore, when C/N was in the range of 10–15, the biological activity and the granulation were excellent; therefore, the adsorption performance and the microbial assimilation ability were better than those of the P2-R3 and P2-R4 groups. Collectively, these results suggest that the TP removal efficiency was better when C/N was 10–15.

3.3. Recyclability Analysis

The high-temperature sodium carbonate method was used for the efficient recycling of SA by recovering SA from the granules or nongranular sludge of each group. The content of SA that could be extracted and recovered is shown in Figure 13. The results showed that there was a significant difference in the content of recoverable SA among groups, where the lowest was 27% and the highest was 85%. Combining the granulation and EPS content of AGS in the P1 and P2 systems during the mature period, the AGS group with a complete structure and excellent sedimentation performance generally had a higher recovery efficiency of SA compared with the group that could not form granular sludge. In addition, in the group that could form granular sludge, the recovery efficiency of SA was positively correlated with PN/PS. The results suggested that the more PS in EPS, the stronger the hydrophilicity of sludge, and the compatibility of sludge particles with water increased, thereby resulting in a loose surface, decreased sedimentation performance, and poor granulation effect. At the same time, this made it more difficult for the high-temperature sodium carbonate method to destroy the sludge structure and extract SA, and, consequently, the recovery efficiency of SA decreased.

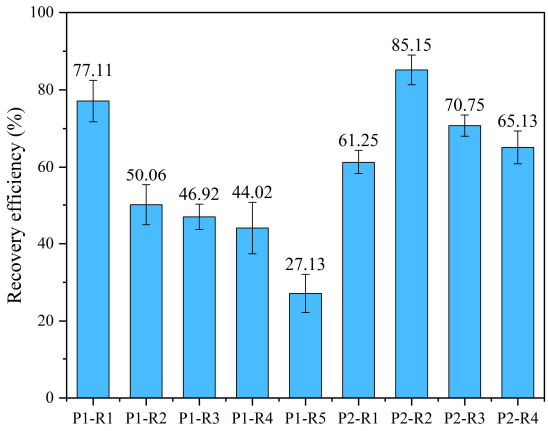

Figure 13. Recovery efficiency of SA in excess activated sludge.

According to the findings of this study, maintaining an optimal OLR and C/N ratio within suitable ranges can promote the rapid formation of stable AGS driven by a SAN. Therefore, considering the crucial significance of shortening granulation time and enhancing granular stability, we recommend controlling the OLR and C/N ratio by blending raw piggery flushing wastewater with pre-sedimentation tank effluent of piggery flushing wastewater in varying proportions ranging from 1.4 to 2.4 kg/(m^3·d) and 10 to 15, respectively. However, it is important to acknowledge that long-term operation may disrupt the dynamic equilibrium between disintegration and regranulation in AGS, leading to alterations in removal performance and granular characteristics. Unfortunately, this study solely focuses on investigating the impact of the OLR and C/N ratio on AGS formation

and performance using a SAN as a carrier core for only a half-month experimental period. Therefore, for successful implementation at large-scale engineering applications, further research examining the long-term performance of AGS utilizing a SAN as a carrier core is imperative.

4. Conclusions

In the present study, different OLR and C/N experiments were designed to explore the granulation effect of AGS with a SAN, followed by an analysis of the structure and performance of the formed AGS. The results showed that AGS with a stable structure and excellent performance could be effectively formed when the OLR in the reactor with the addition of a SAN was controlled within the range of 1.4–2.4 kg/(m^3·d). The influence of different OLRs on AGS granulation mainly depended on the types of AGS microorganisms. Under lower OLR levels, the AGS was mainly rod-shaped and spherical bacteria. With an increase in the OLR, the proportion of filamentous bacteria increased. Moreover, when C/N was controlled in the range of 10–15, AGS with uniform particle size and excellent performance could be formed. The influence of different C/N ratios on the granulation and performance was mainly dependent on microbial activity. A too low C/N caused insufficient nutrients and low microbial activity, whereas a high C/N made the nitrogen source deficient, and autotrophic nitrifying bacteria could become the dominant species; therefore, the granulation and performance were poor.

Author Contributions: Conceptualization, C.G., Q.C. and Y.C. (Yao Chen); methodology, C.G., Q.C. and R.C.; software, Y.C. (Ying Chen) and Y.W.; formal analysis, C.G., Q.C. and X.C.; investigation, R.C., X.C. and Y.C. (Ying Chen); data curation, X.C. and Y.W.; writing—original draft preparation, C.G. and Q.C.; writing—review and editing, C.L. and Y.C. (Yao Chen); visualization, R.C. and Y.C. (Ying Chen); supervision, Y.C. (Yao Chen); project administration, Y.C. (Yao Chen); funding acquisition, S.X. and C.L. All authors have read and agreed to the published version of the manuscript.

Funding: This work was funded by the Scientific and Technological Research Project of the Chongqing Education Commission (KJQN202000702), the Venture and Innovation Support Program for Chongqing Overseas Returnees (cx2020041), and the Science and Technology Project of Chongqing Design Group Co., Ltd. (2023-B8).

Data Availability Statement: The data used in this study are available upon request.

Conflicts of Interest: Author Chunjuan Gan, Xi Chen, Yizhou Wu, and Shanchuan Xu were employed by the Municipal Design Research Institute of Chongqing Design Group Co. Ltd. The remaining authors declare that the research was conducted in the absence of any commercial or financial relationships that could be construed as a potential conflict of interest.

References

1. Hussain, S.; Ferrentino, R.; Khan, K.; Ali, Z.; Yousuf, M.; Andreottola, G. Rapid startup of aerobic granular sludge: Recent advances and future challenges. *Results Eng.* **2024**, *22*, 102035. [CrossRef]
2. Xu, D.; Li, J.; Qu, X.; Ma, H. Advances in continuous flow aerobic granular sludge: A review. *Process Saf. Environ.* **2022**, *163*, 27–35. [CrossRef]
3. Iorhemen, O.T.; Liu, Y. Effect of feeding strategy and organic loading rate on the formation and stability of aerobic granular sludge. *J. Water Process Eng.* **2021**, *39*, 101709–101719. [CrossRef]
4. Sarvajith, M.; Nandini, D.; Nancharaiah, Y.V. Comparative evaluation of activated sludge and aerobic granular sludge for biological treatment of real domestic wastewater with oxytetracycline dosing. *J. Environ. Chem. Eng.* **2024**, *12*, 112482. [CrossRef]
5. Carrera, P.; Casero-Díaz, T.; Castro-Barros, C.M.; Méndez, R.; Val del Río, A.; Mosquera-Corral, A. Features of aerobic granular sludge formation treating fluctuating industrial saline wastewater at pilot scale. *J. Environ. Manag.* **2021**, *296*, 113135. [CrossRef] [PubMed]
6. Hou, Y.; Gan, C.; Chen, R.; Chen, Y.; Yuan, S.; Chen, Y. Characteristics of aerobic granular sludge and factors that influence its stability: A mini review. *Water* **2021**, *13*, 2726. [CrossRef]
7. Liu, Z.; Zhang, D.; Yang, R.; Wang, J.; Duan, Y.; Gao, M.; Wang, J.; Zhang, A.; Liu, Y.; Li, Z. Changes and stage disparity of aerobic sludge granulation with increasing organic load rate under low organotrophic conditions. *J. Clean. Prod.* **2024**, *450*, 141937. [CrossRef]

8. Da Costa, R.; Ghobril, C.; Perrin, R.; Sanson, N. Adsorption of sodium alginate on calcium carbonate microparticles: Effect of molar mass and composition. *Colloids Surface A* **2024**, *682*, 132782. [CrossRef]
9. Gao, X.; Guo, C.; Hao, J.; Zhao, Z.; Long, H.; Li, M. Adsorption of heavy metal ions by sodium alginate based adsorbent—A review and new perspectives. *Int. J. Biol. Macromol.* **2020**, *164*, 4423–4434. [CrossRef] [PubMed]
10. Díez-García, I.; Lemma, M.R.D.C.; Barud, H.S.; Eceiza, A.; Tercjak, A. Hydrogels based on waterborne poly(urethane-urea)s by physically cross-linking with sodium alginate and calcium chloride. *Carbohyd. Polym.* **2020**, *250*, 116940. [CrossRef]
11. Wang, B.; Wan, Y.S.; Zheng, Y.L.; Lee, X.Q.; Liu, T.Z.; Yu, Z.B.; Huang, J.; Ok, Y.S.; Chen, J.J.; Gao, B. Alginate-based composites for environmental applications: A critical review. *Crit. Rev. Environ. Sci. Technol.* **2019**, *49*, 318–356. [CrossRef] [PubMed]
12. Covarrubias, S.A.; De-Bashan, L.E.; Moreno, M.; Bashan, Y. Alginate beads provide a beneficial physical barrier against native microorganisms in wastewater treated with immobilized bacteria and microalgae. *Appl. Microbiol. Biotechnol.* **2012**, *93*, 2669–2680. [CrossRef] [PubMed]
13. Tang, Y.; Wu, Q.; Chen, Y.; Liu, Z.; Chen, Y.; Chen, R.; Wu, Q.; Ren, B.; Li, C. Addition of sodium alginate as a nucleus shortens granulation of aerobic sludge. *Environ. Sci.-Water Res. Technol.* **2022**, *8*, 2216. [CrossRef]
14. Moy, B.Y.; Tay, J.H.; Toh, S.K.; Liu, Y.; Tay, S.T. High organic loading influences the physical characteristics of aerobic sludge granules. *Lett. Appl. Microbiol.* **2010**, *34*, 407–412. [CrossRef] [PubMed]
15. Corsino, S.F.; Trapani, D.D.; Torregrossa, M.; Viviani, G. Aerobic granular sludge treating high strength citrus wastewater: Analysis of pH and organic loading rate effect on kinetics, performance and stability. *J. Environ. Manag.* **2018**, *214*, 23–35. [CrossRef] [PubMed]
16. Wang, L.; Liu, X.; Li, Z.; Wan, C.; Zhang, Y. Filamentous aerobic granular sludge: A critical review on its cause, impact, control and reuse. *J. Environ. Chem. Eng.* **2023**, *11*, 110039. [CrossRef]
17. Adav, S.S.; Lee, D.J.; Lai, J.Y. Potential cause of aerobic granular sludge breakdown at high organic loading rates. *Appl. Microbiol. Biotechnol.* **2010**, *85*, 1601–1610. [CrossRef] [PubMed]
18. Zheng, Y.M.; Yu, H.Q.; Liu, S.J.; Liu, X.Z. Formation and instability of aerobic granules under high organic loading conditions. *Chemosphere* **2006**, *63*, 1791–1800. [CrossRef] [PubMed]
19. Zhang, Z.; Yu, Z.; Dong, J.; Wang, Z.; Ma, K. Stability of aerobic granular sludge under condition of low influent C/N ratio: Correlation of sludge property and functional microorganism. *Bioresour. Technol.* **2018**, *270*, 391–399. [CrossRef]
20. Li, D.; Guo, W.; Liang, D.; Zhang, J.; Li, J.; Li, P.; Wu, Y.; Bian, X.; Ding, F. Rapid start-up and advanced nutrient removal of simultaneous nitrification, endogenous denitrification and phosphorus removal aerobic granular sequence batch reactor for treating low C/N domestic wastewater. *Environ. Res.* **2022**, *212*, 113464. [CrossRef]
21. Meng, J.; Li, J.; Li, J.; Antwi, P.; Deng, K.; Wang, C.; Buelna, G. Nitrogen removal from low COD/TN ratio manure-free piggery wastewater within an upflow microaerobic sludge reactor. *Bioresour. Technol.* **2015**, *198*, 884–890. [CrossRef]
22. Luo, J.; Hao, T.; Wei, L.; Mackey, H.R.; Lin, Z.; Chen, G.H. Impact of influent COD/N ratio on disintegration of aerobic granular sludge. *Water Res.* **2014**, *62*, 127–135. [CrossRef]
23. Sarv Aj Ith, M.; Reddy, G.; Nancharaiah, Y.V. Aerobic granular sludge for high-strength ammonium wastewater treatment: Effect of COD/N ratios, long-term stability and nitrogen removal pathways. *Bioresour. Technol.* **2020**, *306*, 123150–123160. [CrossRef]
24. Wang, X.; Wang, S.; Xue, T.; Li, B.; Dai, X.; Peng, Y. Treating low carbon/nitrogen (C/N) wastewater in simultaneous nitrification-endogenous denitrification and phosphorous removal (SNDPR) systems by strengthening anaerobic intracellular carbon storage. *Water Res.* **2015**, *77*, 191–200. [CrossRef] [PubMed]
25. Derlon, N.; Wagner, J.; da Costa, R.H.R.; Morgenroth, E. Formation of aerobic granules for the treatment of real and low-strength municipal wastewater using a sequencing batch reactor operated at constant volume. *Water Res.* **2016**, *105*, 341–350. [CrossRef] [PubMed]
26. Yang, Y.; Peng, Y.; Cheng, J.; Zhang, S.; Liu, C.; Zhang, L. A novel two-stage aerobic granular sludge system for simultaneous nutrient removal from municipal wastewater with low C/N ratios. *Chem. Eng. J.* **2023**, *462*, 142318. [CrossRef]
27. Li, J.; Deng, K.; Li, J.; Liu, M.; Meng, J. Nitrogen removal and bacterial mechanism in a hybrid anoxic/oxic baffled reactor affected by shortening HRT in treating manure-free piggery wastewater. *Int. Biodeterior. Biodegrad.* **2021**, *163*, 105284. [CrossRef]
28. Tian, Y.; Li, J.; Fan, Y.; Li, J.; Meng, J. Performance and nitrogen removal mechanism in a novel aerobic-microaerobic combined process treating manure-free piggery wastewater. *Bioresour. Technol.* **2022**, *345*, 126494. [CrossRef]
29. Zhao, H. *The Two-Stage Anaerobic Digestion—Subsurface Flow Wetland Process for the Courtyard Sewage Treatment in South Hilly Area*; Chinese Research Academy of Environmental Sciences: Beijing, China, 2013.
30. Sajjad, M.; Kim, K.S. Studies on the interactions of Ca^{2+} and Mg^{2+} with EPS and their role in determining the physicochemical characteristics of granular sludges in SBR system. *Process Biochem.* **2015**, *50*, 966–972. [CrossRef]
31. APHA. *Standard Methods for the Examination of Water and Wastewater*; Public Health Association: Washington, DC, USA, 2005.
32. Zhang, Z.; Qiu, J.; Xiang, R.; Yu, H.; Xu, X.; Zhu, L. Organic loading rate (OLR) regulation for enhancement of aerobic sludge granulation: Role of key microorganism and their function. *Sci. Total Environ.* **2018**, *653*, 630–637. [CrossRef]
33. Xia, J.; Ye, L.; Ren, H.; Zhang, X. Microbial community structure and function in aerobic granular sludge. *Appl. Microbiol. Biotechnol.* **2018**, *102*, 3967–3979. [CrossRef] [PubMed]
34. Chen, Y.; Zhu, Z.; Yu, W.; Zhang, C. Granulation process and mechanism of aerobic granular sludge under salt stress in a sequencing batch reactor. *Tecnol. Cienc. Agua* **2019**, *10*, 156–181. [CrossRef]

35. Figueroa, M.; Val del Río, A.; Campos, J.L.; Méndez, R.; Mosquera-Corral, A. Filamentous bacteria existence in aerobic granular reactors. *Bioprocess Biosyst. Eng.* **2015**, *38*, 841–851. [CrossRef] [PubMed]
36. Long, B.; Xuan, X.; Yang, C.; Zhang, L.; Cheng, Y.; Wang, J. Stability of aerobic granular sludge in a pilot scale sequencing batch reactor enhanced by granular particle size control. *Chemosphere* **2019**, *225*, 460–469. [CrossRef] [PubMed]
37. Long, B.; Yang, C.Z.; Pu, W.H.; Yang, J.K.; Liu, F.B.; Zhang, L.; Zhang, J.; Cheng, K. Tolerance to organic loading rate by aerobic granular sludge in a cyclic aerobic granular reactor. *Bioresour. Technol.* **2015**, *182*, 314–322. [CrossRef] [PubMed]
38. Show, K.Y.; Lee, D.J.; Tay, J.H. Aerobic Granulation: Advances and Challenges. *Appl. Biochem. Biotechnol.* **2012**, *167*, 1622–1640. [CrossRef] [PubMed]
39. Sun, H.; Yu, P.; Li, Q.; Ren, H.; Liu, B.; Ye, L.; Zhang, X.-X. Transformation of anaerobic granules into aerobic granules and the succession of bacterial community. *Appl. Microbiol. Biotechnol.* **2017**, *101*, 7703–7713. [CrossRef] [PubMed]
40. Li, Y.; Shen, L.; Chen, F. DO diffusion profile in aerobic granule and its microbiological implications. *Enzym. Microb. Technol.* **2008**, *43*, 349–354. [CrossRef]
41. Verawaty, M.; Tait, S.; Pijuan, M.; Yuan, Z.; Bond, P.L. Breakage and growth towards a stable aerobic granule size during the treatment of wastewater. *Water Res.* **2013**, *47*, 5338–5349. [CrossRef]
42. Zhu, L.; Lv, M.; Dai, X.; Yu, Y.; Qi, H.; Xu, X. Role and significance of extracellular polymeric substances on the property of aerobic granule. *Bioresour. Technol.* **2012**, *107*, 46–54. [CrossRef]
43. Peng, T.; Wang, Y.; Wang, J.; Fang, F.; Yan, P.; Liu, Z. Effect of different forms and components of EPS on sludge aggregation during granulation process of aerobic granular sludge. *Chemosphere* **2022**, *303*, 135116. [CrossRef] [PubMed]
44. Wang, Y.; Wang, J.; Liu, Z.; Huang, X.; Fang, F.; Guo, J.; Yan, P. Effect of EPS and its forms of aerobic granular sludge on sludge aggregation performance during granulation process based on XDLVO theory. *Sci. Total Environ.* **2021**, *795*, 148682. [CrossRef] [PubMed]
45. Seviour, T.; Yuan, Z.; Loosdrecht, M.; Lin, Y. Aerobic sludge granulation: A tale of two polysaccharides? *Water Res.* **2012**, *46*, 4803–4813. [CrossRef] [PubMed]
46. Liu, Y.; Wei, D.; Xu, W.; Feng, R.; Wei, Q. Nitrogen removal in a combined aerobic granular sludge and solid-phase biological denitrification system: System evaluation and community structure. *Bioresour. Technol.* **2019**, *288*, 121504–121511. [CrossRef] [PubMed]
47. Bassin, J.P.; Kleerebezem, R.; Dezotti, M.; Van Loosdrecht, M.C.M. Measuring biomass specific ammonium, nitrite and phosphate uptake rates in aerobic granular sludge. *Chemosphere* **2012**, *89*, 1161–1168. [CrossRef] [PubMed]
48. Bassin, J.P.; Tavares, D.C.; Borges, R.C.; Dezotti, M. Development of aerobic granular sludge under tropical climate conditions: The key role of inoculum adaptation under reduced sludge washout for stable granulation. *J. Environ. Manag.* **2018**, *230*, 168–182. [CrossRef] [PubMed]
49. Coma, M.; Verawaty, M.; Pijuan, M.; Yuan, Z.; Bond, P.L. Enhancing aerobic granulation for biological nutrient removal from domestic wastewater. *Bioresour. Technol.* **2012**, *103*, 101–108. [CrossRef] [PubMed]
50. Xin, X.; Qin, J. Rapid start-up of partial nitritation in aerobic granular sludge bioreactor and the analysis of bacterial community dynamics. *Bioprocess Biosyst. Eng.* **2019**, *42*, 1973–1981. [CrossRef] [PubMed]
51. Mlinar, S.; Weig, A.R.; Freitag, R. Influence of NH_3 and NH_4^+ on anaerobic digestion and microbial population structure at increasing total ammonia nitrogen concentrations. *Bioresour. Technol.* **2022**, *361*, 127638. [CrossRef]
52. Zhou, J.H.; Zhang, Z.M.; Zhao, H.; Yu, H.T.; Alvarez, P.; Xu, X.Y.; Zhu, L. Optimizing granules size distribution for aerobic granular sludge stability: Effect of a novel funnel-shaped internals on hydraulic shear stress. *Bioresour. Technol.* **2016**, *216*, 562–570. [CrossRef]
53. Gül, G.A.; Ferhan, Ç. Production of protein- and carbohydrate-EPS in activated sludge reactors operated at different carbon to nitrogen ratios. *J. Chem. Technol. Biotechnol.* **2016**, *91*, 522–531.
54. Chen, Z.; Wang, X.; Zhou, S.; Fan, J.; Chen, Y. Large-scale (500 kg N/day) two-stage partial nitritation/anammox (PN/A) process for liquid-ammonia mercerization wastewater treatment: Rapid start-up and long-term operational performance. *J. Environ. Manag.* **2023**, *326*, 116404. [CrossRef] [PubMed]
55. Sun, G.; Zhu, Y.; Saeed, T.; Zhang, G.; Lu, X. Nitrogen removal and microbial community profiles in six wetland columns receiving high ammonia load. *Chem. Eng. J.* **2012**, *203*, 326–332. [CrossRef]
56. He, Q.; Chen, L.; Zhang, S.; Chen, R.; Wang, H. Hydrodynamic shear force shaped the microbial community and function in the aerobic granular sequencing batch reactors for low carbon to nitrogen (C/N) municipal wastewater treatment. *Bioresour. Technol.* **2018**, *271*, 48–58. [CrossRef] [PubMed]